Earthquakes and Structures, Vol. 3, No. 3-4 (2012) 271-295
DOI: http://dx.doi.org/10.12989/eas.2012.3.3.271

Dynamic analysis of a cable-stayed bridge using continuous formulation of 1-D linear member

Chih-Peng Yu* and Chia-Chi Cheng

Department of Construction Engineering, Chaoyang University of Technology, 168 Gifeng E. Rd., Wufeng, Taiwan

(Received December 6, 2011, Revised January 2, 2012, Accepted February 10, 2012)

Abstract. This paper presents the solution scheme of using the continuous formulation of 1-D linear member for the dynamic analysis of structures consisting of axially loaded members. The context describes specific applications of such scheme to the verification of experimental data obtained from field test of bridges carried out by a microwave interferometer system and velocimeters. Attention is focused on analysis outlines that may be applicable to in-situ assessment for cable-stayed bridges. The derivation of the dynamic stiffness matrix of a prismatic member with distributed properties is briefly reviewed. A back calculation formula using frequencies of two arbitrary modes of vibration is next proposed to compute the tension force in cables. Derivation of the proposed formula is based on the formulation of an axially loaded flexural member. The applications of the formulation and the proposed formula are illustrated with a series of realistic examples.

Keywords: dynamic stiffness matrix; axially loaded member; cable force; cable-stayed bridge; transfer function

1. Introduction

Due to their high efficiency in utilizing the prestressing forces, most cable-stayed bridges consist of slender members with regular cross sections. Thus, bridges of this type and their variations, including the so-called extradosed bridges, can normally be modeled using 1-D line elements as a combination of simplified frame structures and tensioned cables. Depending on the types of excitations and responses associated with the analysis task, analysis of cable-stayed bridges can be carried out with either a nonlinear or a linear solution scheme. For dynamic problems associated with responses due to non-destructive testing (NDT) tests and ambient vibrations, bridges can normally be reasonably represented by a linear model since the fluctuations caused by these excitations are considered to be relatively insignificant to the initial static responses. Dynamic analysis of cable-stayed bridges can be properly carried out using finite element (FE) techniques with discrete formulation in the time domain. With the help of versatile FEM packages, time domain scheme has been widely adopted. For example, recent relevant references include Bhagwat *et al*. (2011) demonstrated the use of ANSYS to investigate the seismic responses of cable-stayed bridges, and Ali and Okabayashi (2011) proposed a system identification scheme for bridges in

*Corresponding author, Associate Professor, E-mail: cpyu@cyut.edu.tw

which useful numerical simulations can be generated by simple 1-D FEM models. Except for cases including significant behavior associated with slack cables, the use of a continuous formulation with distributed properties in the frequency domain, however, provides a more efficient and sometimes even more accurate procedure for the linearly dynamic analysis of frames than the lumped or consistent formulations.

Over the past decades, the dynamic stiffness matrices for various continuous members have been extensively investigated and independently used to study different problems by different researchers (e.g. Latona 1969, Papaleontiou 1992, Banerjee and William 1994, Doyle 1997, Yu 1992, 1996, Dai 2005). Recent references related to this article include, for instance, Dai *et al*. (2007) which thoroughly discussed the general applications of such dynamic stiffness matrices to dynamic and wave propagation problems, and Yu and Roesset (2001) in which the general formulation for 1-D prismatic members with respect to various theories were systematically summarized. Since stay cables and prestressed box girders are axially loaded members, the formulation including the effect due to axial force is of particular interest and would thus be outlined in this paper.

Regarding the dynamics of tensioned slender members, tension force of a cable can be practically calculated with the first natural frequency based on theory of a vibrating string. However, tension forces based on the simple string theory are often overestimated and could be quite inaccurate for certain cases. The major reason is that the lack of considerations of effects associated with flexural stiffness and end constraints leads to the inadequacy in correctly describing the transverse vibration (Wenzel and Pichler 2005). As a result, formulas based on the axially loaded beam provide better approximations for the dynamic characteristics of tensioned cables. When considering directly applying such formulas to assess cable forces, there is one important parameter needed to be recognized beforehand, namely the flexural stiffness. Although structural properties of most cable systems should practically be known values, precise information for certain stay cables may not be possible due to their intricacy in composition. To overcome the above difficulty, a systematic derivation for the dynamic responses of a general flexural member were thoroughly reviewed by the authors and a series of feasible formulas which can be used with field data to predict reasonable values of length/axial force/rigidity were studied and verified with test data (Yu *et al*. 2011). It is of particular interest to the authors to demonstrate, in this paper, a useful formula for computing the cable force from two natural frequencies without the need of precisely knowing the flexural rigidity.

Owing to its distinguishing features of high accuracy and non-contact, the microwave interferometer has gradually become popular and used for monitoring the dynamic characteristics of the bridge decking system and the cables. Cheng *et al*. (2010) used IBIS-S, which is an instrument carrying microwave sensors and has a 1-D imaging capability for remotely measuring the displacements of multiple locations simultaneously, to monitor the dynamic behavior of various types of bridges. It was concluded that such device can be a proper tool for speedy, accurate and non-contact measurement of the dynamic response of a wide range of bridge structures with an average setup time less than 30 minutes. By equipping the measurement system with an efficient computer program for structural analysis to enable the in-situ verification, the use of a microwave interferometer was found to have the potential to serve as an efficient scheme for the quick assessment of bridges.

The paper is aimed to introduce a simple yet complete strategy for carrying out the linear dynamic analysis of a cable-stayed bridge and to outline the related theoretic backgrounds. First, the derivation of dynamic stiffness matrix is briefly reviewed with emphasis on the formulation related to axially loaded members. The context of deriving an improved equation used in recovering cable forces is next introduced. Typical results of the simulated bridge using the continuous formulation are illustrated with numerical examples and their applications to help verify the field data.

2. Dynamic stiffness matrices

As mentioned above, the details regarding derivations of dynamic stiffness matrices of the 1-D continuous member can be found in references (Dai *et al.* 2007, Yu and Roesset 2001). The derivation scheme of dynamic stiffness matrix, however, is still briefly outlined in this section for providing completeness of the context. Despite that dynamic stiffness matrix can be numerically obtained, explicit form associated with simpler theories can be use to obtain useful analytical expression of simple problems and can potentially provide insightful information, thus the derivation of such simpler explicit form is also presented.

2.1 Axially loaded Rayleigh beam

Consider a uniform member subjected to a constant axial force N with Young's modulus E, cross-sectional area A, moment of inertia I and mass density ρ. The governing equation in the frequency domain for the transverse vibrations of the member using the Rayleigh beam theory and including effects of axial load and rotational inertia are

$$\frac{\partial \hat{M}}{\partial x} + \hat{V} = -\omega^2 \rho I \hat{v}' \tag{1a}$$

$$\frac{\partial \hat{Y}}{\partial x} = -\omega^2 \rho A \hat{v} \tag{1b}$$

$$\hat{M} = EI\hat{v}'' \tag{1c}$$

$$\hat{Y} = \hat{V} + N\hat{v}'' \tag{1d}$$

where $\hat{M}$, $\hat{Y}$, $\hat{V}$ and $\hat{v}$ represent, in the frequency domain, the bending moment, vertical force, shear force of the cross section and transverse displacement of the centroidal axis. A positive N represents a tension force. The assumption of constant N implies that the fluctuation due to dynamic loads are much less than the original static axial force. Combining the above equations gives then

$$EI\hat{v}^{IV} + [\omega^2 \rho I - N]\hat{v}'' - \omega^2 \rho A \hat{v} = 0 \tag{2}$$

By defining

$$2\beta = \frac{\omega^2 \rho I - N}{EI} \text{ and } \alpha^2 = \frac{\omega^2 \rho A}{EI} \tag{3}$$

The solution of Eq. (2) can be expressed as

$$\hat{v} = C_1 e^{r_1 x} + C_2 e^{r_2 x} + C_3 e^{r_3 x} + C_4 e^{r_4 x} \tag{4}$$

where r_1, r_2, r_3 and r_4 are the roots of the characteristic equation

$$r^4 + 2\beta r^2 - \alpha^2 = 0 \tag{5}$$

To form the dynamic stiffness matrix, we first express end displacement $\{\hat{u}\}$ in terms of the constant C_i as

$$\{\hat{u}\} = \{\hat{v}(0)\ \ \hat{v}'(0)\ \ \hat{v}(L)\ \ \hat{v}'(L)\}^T = [T_1]\{C_1\ \ C_2\ \ C_3\ \ C_4\}^T = [T_1]\{C\} \tag{6}$$

and end force $\{\hat{F}\}$ in terms of the constant C_i as

$$\{\hat{F}\} = \{-\hat{Y}(0)\ \ -\hat{M}(0)\ \ \hat{Y}(L)\ \ \hat{M}(L)\}^T = [T_2]\{C_1\ \ C_2\ \ C_3\ \ C_4\}^T = [T_2]\{C\} \tag{7}$$

Since $\{\hat{F}\} = [T_2]\{C\} = [T_2][T_1]^{-1}\{\hat{u}\} = [S_f]\{\hat{u}\}$, the computation of the stiffness matrix $\lfloor S_f \rfloor$ can be numerically performed as

$$[S_f] = [T_2][T_1]^{-1} \tag{8}$$

Alternatively, the explicit form of the stiffness matrix $\lfloor S_f \rfloor$ can be derived. For the reason of simplicity in derivation, the solution form is changed to $\hat{v} = \overline{C}_1 \sin\sigma x + \overline{C}_2 \cos\sigma x + \overline{C}_3 \sinh\varepsilon x + \overline{C}_4 \cosh\varepsilon x$

with

$$\sigma^2 = \beta + \sqrt{\beta^2 + \alpha^2} \ \text{ and } \ \varepsilon^2 = -\beta + \sqrt{\beta^2 + \alpha^2} \tag{9}$$

The two coefficient matrices can thus be obtained as

$$[T_1] = \begin{bmatrix} 0 & 1 & 0 & 1 \\ \sigma & 0 & \varepsilon & 0 \\ s & c & SH & CH \\ \sigma c & -\sigma s & \varepsilon CH & \varepsilon SH \end{bmatrix},\ [T_2] = EI \begin{bmatrix} -\alpha^2/\sigma & 0 & \alpha^2/\varepsilon & 0 \\ 0 & \sigma^2 & 0 & -\varepsilon^2 \\ \alpha^2 c/\sigma & -\alpha^2 s/\sigma & -\alpha^2 SH/\varepsilon & -\alpha^2 CH/\varepsilon \\ -\sigma^2 s & -\sigma^2 c & \varepsilon^2 SH & \varepsilon^2 CH \end{bmatrix}$$

$$\text{with } [T_1]^{-1} = \frac{1}{\Delta} \begin{bmatrix} -\varepsilon(\varepsilon cSH + \sigma\varepsilon CH) & \varepsilon(1 - cCH) - \sigma sSH & \varepsilon(\varepsilon SH + \sigma s) & \varepsilon(c - CH) \\ \sigma\varepsilon(1 - cCH) + \varepsilon^2 sSH & \varepsilon sCH - \sigma cSH & \sigma\varepsilon(c - CH) & \sigma SH - \varepsilon s \\ \sigma(\varepsilon cSH + \sigma sCH) & \sigma(1 - cCH) - \varepsilon sSH & -\sigma(\varepsilon SH + \sigma s) & \sigma(CH - c) \\ \sigma\varepsilon(1 - cCH) - \sigma^2 sSH & -\varepsilon sCH + \sigma cSH & \sigma\varepsilon(CH - c) & -\sigma SH + \varepsilon s \end{bmatrix},$$

in which s, c, SH and CH stand for $\sin\sigma L$, $\cos\sigma L$, $\sinh\varepsilon L$ and $\cosh\varepsilon L$, respectively, and $\Delta = 2\sigma\varepsilon[1\text{-}cCH] + (\varepsilon^2 - \sigma^2)sSH$.

Carrying out the matrix multiplication, the dynamic stiffness matrix can be expressed as

$$[S_f] = \frac{EI}{\Delta} \times \begin{bmatrix} S_{11} & S_{12} & S_{13} & S_{14} \\ & S_{22} & S_{23} & S_{24} \\ & & S_{33} & S_{34} \\ sym & & & S_{44} \end{bmatrix} \tag{10}$$

with $S_{11} = \sigma\varepsilon(\sigma^2 + \varepsilon^2) \times (\sigma\varepsilon CH + \varepsilon cSH)$

$S_{12} = \sigma\varepsilon(\sigma^2 - \varepsilon^2)(1 - cCH) + 2\sigma^2\varepsilon^2 sSH$

$S_{13} = -\sigma\varepsilon(\sigma^2 + \varepsilon^2) \times (\sigma s + \varepsilon SH)$

$S_{14} = -\sigma\varepsilon(\sigma^2 + \varepsilon^2) \times (c - CH)$

$S_{22} = (\sigma^2 + \varepsilon^2) \times (\sigma cSH - \varepsilon sCH)$

$S_{23} = -S_{14}$

$S_{24} = (\sigma^2 + \varepsilon^2) \times (\sigma SH - \varepsilon s)$

$S_{33} = S_{11}$, $S_{34} = -S_{12}$, $S_{44} = S_{22}$

2.2 General linear element

2.2.1 Transverse vibration

In addition to the basic effects accounting for in the axially loaded Rayleigh beam element, the most general case for the flexural element would also include effects due to shear deformation (i.e., Timoshenko beam) and distributed springs (due to soil pile interaction). Referring to Fig. 1, the corresponding governing equations can be expressed as in Eq. (11)

$$\frac{\partial \hat{M}}{\partial x} + \hat{V} = -\rho I\omega^2\hat{\varphi} + k_r\hat{\varphi} + c_r\dot{\hat{\varphi}} = -(\rho I\omega^2 - K_r)\hat{\varphi} = -D_r\hat{\varphi} \tag{11a}$$

$$\frac{\partial \hat{Y}}{\partial x} = -\rho A\omega^2\hat{v} + k_f\hat{v} + c_f\dot{\hat{v}} = -(\rho A\omega^2 - K_f)\hat{v} = -D_f\hat{v} \tag{11b}$$

$$\hat{M} = EI\hat{\varphi}' \tag{11c}$$

$$\hat{Y} = \hat{V} + N\hat{v}' = [\kappa GA(\hat{v}' - \hat{\varphi})] + N\hat{v}' \tag{11d}$$

in which, $\hat{\varphi}$ is rotation of the cross section, κ and G are effective shear area coefficient and Shear Modulus, K_f and K_r are the dynamic stiffness functions with $K = k + i\omega c$, standing for the restraining effects in the transverse and bending rotational directions, respectively. In the above equations, D_f and D_r are defined and used to simplify the expressions of the equations. Except for a special case where $\kappa GA = \rho I\omega^2$, the characteristic equation $r^4 + 2\beta r^2 - \alpha^2 = 0$ of this general model becomes

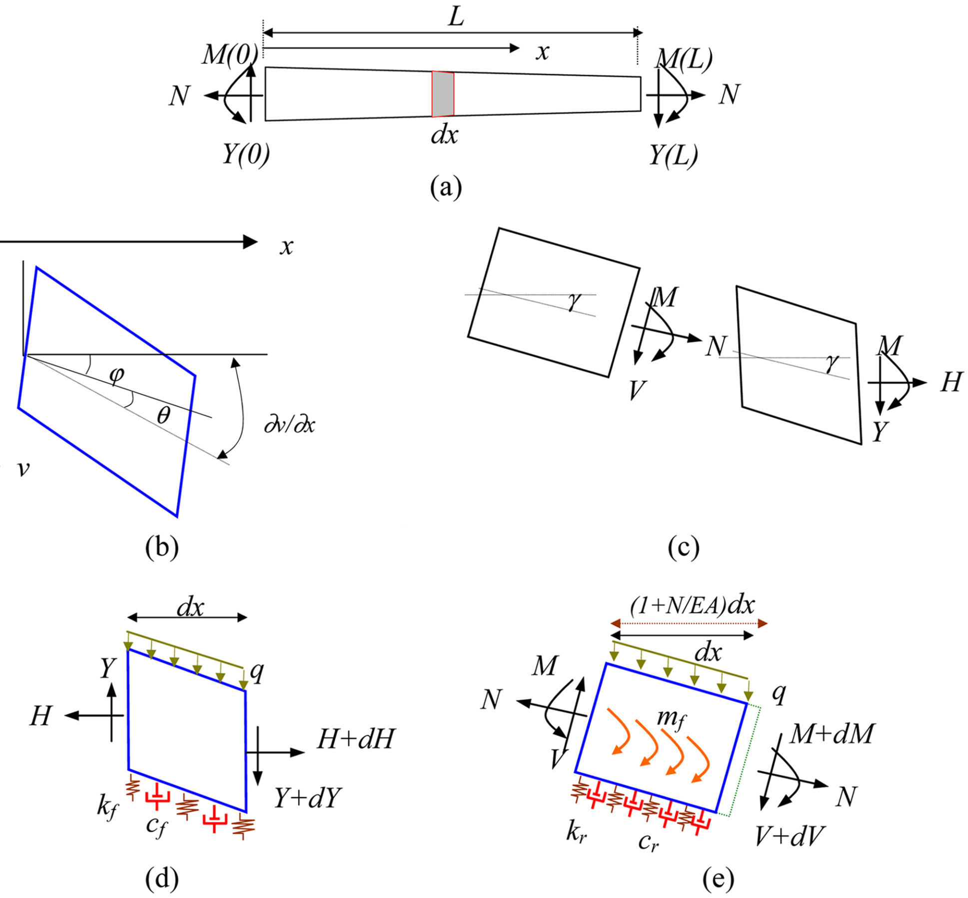

Fig. 1 Differential element for flexural vibration: (a) schematic plot for a flexural member, (b) coordinates and displacements, (c) two pairs of the section forces, (d) equilibrium of transverse forces and (e) equilibrium of bending moments

$$EI\left(1+\frac{N}{\kappa GA}\right)\hat{v}^{IV}+\left[\frac{EI}{\kappa GA}D_f-N+D_r\left(1+\frac{N}{\kappa GA}\right)\right]\hat{v}''-D_f\left[1-\frac{D_r}{\kappa GA}\right]\hat{v}=0 \tag{12}$$

thus, the two terms β and α change to

$$2\beta=\frac{\kappa GA}{(\kappa GA+N)}\left(\frac{D_f}{\kappa GA}-\frac{N}{EI}\right)+\frac{D_r}{EI} \text{ and } \alpha^2=\frac{\kappa GA}{(\kappa GA+N)}\left(\frac{D_f}{EI}\left(1-\frac{D_r}{\kappa GA}\right)\right) \tag{13}$$

The roots are

$$\begin{aligned} r_1 &= -r_2 = \sqrt{-\beta+\sqrt{\beta^2+\alpha^2}} \\ r_3 &= -r_4 = \sqrt{-\beta-\sqrt{\beta^2+\alpha^2}} \end{aligned} \tag{14}$$

Based on Eqs. (6) and (7), the coefficient matrices $[T_1]$ and $[T_2]$ can be expressed as

$$[T_1] = \begin{bmatrix} 1 & 1 & 1 & 1 \\ R_1 & R_2 & R_3 & R_4 \\ e^{r_1 L} & e^{r_2 L} & e^{r_3 L} & e^{r_4 L} \\ R_1 e^{r_1 L} & R_2 e^{r_2 L} & R_3 e^{r_3 L} & R_4 e^{r_4 L} \end{bmatrix} \tag{15}$$

$$[T_2] = \begin{bmatrix} D_f/r_1 & D_f/r_2 & D_f/r_3 & D_f/r_4 \\ -EIR_1 r_1 & -EIR_2 r_2 & -EIR_3 r_3 & -EIR_4 r_4 \\ -D_f e^{r_1 L}/r_1 & -D_f e^{r_2 L}/r_2 & -D_f e^{r_3 L}/r_3 & -D_f e^{r_4 L}/r_4 \\ EIR_1 r_1 e^{r_1 L} & EIR_2 r_2 e^{r_2 L} & EIR_3 r_3 e^{r_3 L} & EIR_4 r_4 e^{r_4 L} \end{bmatrix} \tag{16}$$

in which $R_i = \left[\frac{(\kappa GA + N)}{\kappa GA} r_i + \frac{D_f}{\kappa GA} \frac{1}{r_i}\right]$ and $D_f = (\rho A \omega^2 - K_f)$

The stiffness matrix $\lfloor S_f \rfloor$ can thus be numerically obtained in a straightforward way, while the explicit form for $\lfloor S_f \rfloor$ can be deduced as shown in Yu and Roesset (2001), it is too cumbersome to be useful in providing analytical expressions for simple dynamic problems.

2.2.2 Axial and torsional vibrations

The basic governing equations for axial and torsional vibrations in the frequency domain are respectively

$$(EA\hat{u}')' = -(\rho A \omega^2 \hat{u} - K_a \hat{u}) \tag{17}$$

and

$$(GJ\theta')' = -(\rho I_P \omega^2 \theta - K_T \theta) \tag{18}$$

in which $\hat{u}$ and $\hat{\theta}$ stand for axial displacement and torsional angle in the frequency domain, and A and I_P are the cross sectional area and polar moment of inertia, E and GJ are Young's modulus and torsional rigidity. $K_a(\omega) = k_a(\omega) + i\omega c_a(\omega)$ and $K_T(\omega) = k_T(\omega) + i\omega c_T(\omega)$ represent the dynamic stiffness functions due to the soil-pile interaction. Similar to the flexural stiffness matrix, the axial stiffness matrix can be derived as below;

For a prismatic member with uniform physical properties, Eq. (17) turns into

$$\hat{u}'' + \frac{(\rho A \omega^2 - K_a)}{EA} \hat{u} = 0 \tag{19}$$

The characteristic equation is then in the form as $r^2 + a^2 = 0$ with $a = \sqrt{\frac{(\rho A \omega^2 - K_a)}{EA}}$. The two roots $r_1 = -r_2 = ia$ and the solution form is

$$\hat{u} = C_1 e^{r_1 x} + C_2 e^{r_2 x} \tag{20}$$

Following the same procedure as described from Eqs. (6) to (8), the resulting axial stiffness matrix in the frequency domain can be shown as

$$[S_a] = \frac{iaEA}{e^{iaL} - e^{-iaL}} \begin{bmatrix} e^{iaL} + e^{-iaL} & -2 \\ -2 & e^{iaL} + e^{-iaL} \end{bmatrix} = \frac{aEA}{\sin aL} \begin{bmatrix} \cos aL & -1 \\ -1 & \cos aL \end{bmatrix} \tag{21}$$

with $a = \sqrt{\frac{(\rho A \omega^2 - K_a)}{EA}}$

Similarly the torsional stiffness matrix can be obtained as

$$[S_T] = \frac{iaGJ}{e^{iaL} - e^{-iaL}} \begin{bmatrix} e^{iaL} + e^{-iaL} & -2 \\ -2 & e^{iaL} + e^{-iaL} \end{bmatrix} = \frac{aGJ}{\sin aL} \begin{bmatrix} \cos aL & -1 \\ -1 & \cos aL \end{bmatrix} \tag{22}$$

with $a = \sqrt{\frac{(\rho I_p \omega^2 - K_T)}{GJ}}$

3. Dynamic analyses of cable-stayed bridge

3.1 Stay cables

For the normal cable element without considerations of effects due to gravity and second order geometry, the frequency equations can be expressed as in Eq. (23),

$$f_n = \frac{n}{2L}\sqrt{\frac{N}{\rho A}} \tag{23}$$

in which ρA, N and L are respectively the mass unit length, force and length of the cable with f_n standing for the cyclic frequency of the nth mode of transverse vibration.

It is well known that the axially loaded beam model is superior to the string model in predicting the vibration behavior of slender tensioned cables. Both considerations of flexural rigidity and end constraints help to provide correction terms and lead to better agreement between realistic data and the simulated responses. However, the uncertainty of the flexural rigidity of cables still causes another ambiguous factor in some practical cases. To overcome this problem, the authors developed an alternative formula based on the axially loaded beam model, in which the correction term due to flexural rigidity is replaced by calculating an equivalent string frequency from multiple mode frequencies of the flexural vibration.

To serve as an illustrated example of employing the explicit form of dynamic stiffness matrix in formulating simple dynamic problems, the modal equation of an axially loaded beam with both ends fixed is first derived using the flexural stiffness matrix shown in the previous section. The alternative relation between cable force and natural frequencies is next obtained from the modal equation with certain approximations.

3.1.1 Modal equation by axially loaded beam model

To deduce the modal equation of a fixed-fixed beam from the dynamic stiffness matrix, one can form the stiffness matrix for a two-element member with two equal elements of length $l/2$, namely the left and the right. Since both ends are fixed, the only two kinematic degrees of freedom are the displacement and rotation at the mid-span, denoted as $\hat{v}_{mid}$ and $\hat{\varphi}_{mid}$. Assembling by the direct stiffness approach, the resulting equilibrium equations for the two degree-of-freedom system can then be shown as

$$\begin{bmatrix} \hat{V}_{mid} \\ \hat{M}_{mid} \end{bmatrix} = \frac{EI}{\Delta} \times \begin{bmatrix} S_{33}+S_{11} & S_{34}+S_{12} \\ S_{43}+S_{21} & S_{44}+S_{22} \end{bmatrix} \begin{bmatrix} \hat{v}_{mid} \\ \hat{\varphi}_{mid} \end{bmatrix} = \frac{2EI}{\Delta} \times \begin{bmatrix} S_{11} & 0 \\ 0 & S_{22} \end{bmatrix} \begin{bmatrix} \hat{v}_{mid} \\ \hat{\varphi}_{mid} \end{bmatrix} \tag{24}$$

in which symbols s, c, SH and CH in terms s_{ij} now become $\sin(\sigma l/2)$, $cos(\sigma l/2)$, $\sinh(\varepsilon l/2)$ and $\cosh(\varepsilon l/2)$.

Setting the determinant of the stiffness matrix equal zero to obtain the modal equation, we have $s_{11}s_{22} = \sigma\varepsilon(\sigma^2 + \varepsilon^2)(\sigma sCH + \varepsilon cSH) \times (\sigma^2 + \varepsilon^2)(\sigma cSH - \varepsilon sCH) = 0$

thus

$$(\sigma sCH + \varepsilon cSH) \times (\sigma cSH - \varepsilon sCH) = 0 \tag{25}$$

Expanding and simplifying by double angle formulae lead to the modal frequency equation as

$$\frac{(\sigma^2 - \varepsilon^2)}{2\sigma\varepsilon} = \frac{1 - \cos(\sigma l)\cosh(\varepsilon l)}{\sin(\sigma l)\sinh(\varepsilon l)} \tag{26}$$

The same result can be obtained from traditional approach by separation of variables as can be expected. It is also noted that the modal frequency equation for a simply supported beam of length l can be similarly derived as

$$\sin(\sigma l) = 0 \tag{27}$$

in which non-trivial roots for σl are $n\pi$, $n = 1,2,3,\ldots$

To find out the modal frequencies, Eq. (26) or (27) needs to be solved with the corresponding characteristic equation, Eq. (4). The derivation of the modal frequencies is shown below:
Recall that the characteristic equation is $r^4 + 2\beta r^2 - \alpha^2 = 0$ with two pairs of roots defined by $(\pm i\sigma)^2 = -\sigma^2 = -\beta - \sqrt{\beta^2 + \alpha^2}$ and $(\pm\varepsilon)^2 = \varepsilon^2 = -\beta + \sqrt{\beta^2 + \alpha^2}$. Since rotational inertial term is relatively insignificant for slender tensioned members like normal stay cables, the term $\omega^2 \rho I$ is omitted for simplicity and the two parameters are here defined as

$$2\beta = \frac{-N}{EI} \text{ and } \alpha^2 = \frac{\omega^2 \rho A}{EI} \tag{28}$$

First we define a dimensionless factor δ dominated by the ratio between the slenderness ratio (slr) of the cable and the axial strain (ε), i.e.,

$$\delta = \sqrt{EI/Nl^2} = \sqrt{-2\beta l^2} = \frac{1}{\sqrt{\varepsilon \times slr}} \tag{29}$$

The factor δ can be expected to be small comparing to 1 for normal tensioned cables.
To find out modal frequencies, the characteristic equation, Eq. (4) can be rewritten in terms of σ as

$$(\sigma l)^4 - (2\beta l^2)(\sigma l)^2 - (\alpha l^2)^2 = 0 \tag{30}$$

or, in a form as

$$y^2 = (\alpha l^2)^2 = (-2\beta l^2)(\sigma l)^2 + (\sigma l)^4 = \frac{(\sigma l)^2}{\delta^2} + (\sigma l)^4 \tag{31}$$

in which y is defined to simplify the subsequent procedure. Using the simply supported beam as an example, modal frequencies are solved by substituting σl with $n\pi$. The results are

$$y = \frac{(\sigma l)}{\delta}(1 + (\sigma l)^2\delta^2)^{\frac{1}{2}} = \frac{(n\pi)}{\delta}(1 + (n\pi\delta^2))^{\frac{1}{2}} \tag{32}$$

and thus

$$f_n = \frac{\omega_n}{2\pi} = \left(\frac{n}{2L}\sqrt{\frac{N}{\rho A}}\right) \times \sqrt{1 + (n\pi\delta)^2} \tag{33}$$

in which $\sqrt{1 + (n\pi\delta)^2}$ serves as a correction factor to the mode frequency predicted by the basic string theory. The results for the fixed-fixed beam are more complicated since the roots for Eq. (26) are more difficult to express. To properly approximate the values for σl, we examine the relation between the roots (σ, ε) and the two parameters (β, α) which can clearly be expressed as

$$\sigma\varepsilon = \alpha \text{ and } \sigma^2 - \varepsilon^2 = 2\beta \tag{34}$$

In addition, owing to the fact that $\sinh(\varepsilon l) \cong \cosh(\varepsilon l) >> 1$ holds for the entire range of possible roots, Eq. (26) can thus be reduced to

$$\tan(\sigma l) = \frac{2\sigma\varepsilon}{\varepsilon^2 - \sigma^2} = \left(-\frac{\alpha}{\beta}\right) \tag{35}$$

Using the properties of Taylor expansion, the roots for Eq. (35) can be approximated and expressed as

$$\sigma l = n\pi - \frac{\alpha}{\beta} = n\pi - \frac{\alpha l^2}{\beta l^2} = n\pi + 2\delta^2 y \text{ with } n = 1,2,3,\ldots \tag{36}$$

Plugging Eq. (36) into Eq. (31) and neglecting higher order terms of δ^4, we have a quadratic equation of y as

$$(1-4\delta^2)y^2-[4(n\pi)+8\delta^2(n\pi)^3]y-\left[\frac{(n\pi)^2}{\delta^2}+(n\pi)^4\right]=0 \tag{37}$$

After dropping out the terms higher than third order, the roots for y can then be expressed as

$$y=\frac{(n\pi)}{\delta}\left[(1+2\delta+4\delta^2+8\delta^3)+(n\pi)^2\left(\frac{\delta^2}{2}+4\delta^3\right)\right] \tag{38}$$

As a result, the modal frequencies for a tensioned fixed-fixed beam model can be rigorously approximated by

$$f_n=\frac{\omega_n}{2\pi}=\left(\frac{n}{2L}\sqrt{\frac{N}{\rho A}}\right)\times\left[(1+2\delta+4\delta^2+8\delta^3)+(n\pi)^2\left(\frac{\delta^2}{2}+4\delta^3\right)\right] \tag{39}$$

in which the correction term is clearly more complicated than the previous one for simply supported model. After deriving the frequency equation for vibration modes, it can be applied to provide the relation between cable force and vibration frequency.

3.1.2 relation between cable force and vibration frequency

In the previous section, Eqs. (33) and (39) are expressed in a general form as

$$f_n=f_{n,0}\times\xi_n \tag{40}$$

in which $f_{0,n}=n/2l\sqrt{N/\rho A}$ representing the relation between mode frequency and tension force based on the basic string theory, and ξ_n stands for a correction factor corresponding to the mode frequency of the nth mode. The correction factors in accordance to Eqs. (33) and (39) are respectively shown as

$$\xi_n=\sqrt{1+(n\pi\delta)^2} \tag{41a}$$

$$\xi_n=(1+2\delta+4\delta^2+8\delta^3)+(n\pi)^2\left(\frac{\delta^2}{2}+4\delta^3\right) \tag{41b}$$

with δ defined as $\delta=\sqrt{EI/Nl^2}$.

Both Eqs. (33) and (39) provide better predictions than the traditional string formula when calculating the mode frequency or vice versa the force of tensioned cables. However, to properly use the formulae derived from beam theory, there is still one important parameter needed to be recognized beforehand, namely the flexural stiffness. Certain default factory values may be considered by the testers as given data for specific structural properties, yet precise information may not be possible due to their intricacy in composition. A more versatile formulation which eliminates the use of the flexural stiffness is thus useful to provide testers with alternative ways of verifying estimates for the cable forces.

The proposed way of obtaining such adapted approximation is straight-forward. We start the idea with the simpler case of the simply supported model. Based on the form of Eq. (33), the elimination of the mode related term ($n\pi$) can be achieved by using the squares of two equations expressed at two arbitrary mode frequencies, say f_p^2 and f_n^2 for the pth and nth modes. Subtraction between the two associated equations leads to an alternative expression for the relation between axial force and mode frequencies as shown in Eq. (42)

$$\frac{N}{4l^2\rho A} = \left[\frac{p^4 f_n^2 - n^4 f_p^2}{n^2 p^2 (p^2 - n^2)}\right] \equiv \bar{f}_C^2 \tag{42}$$

By defining an equivalent fundamental frequency of cable vibration, $\bar{f}_C^2$, Eq. (42) demonstrates that Eq. (33) can be transformed into the original form of Eq. (23) without knowing the exact value of the stiffness term. Following a similar procedure used for the fixed-fixed beam model, the resulting equation for Eq. (39) is

$$\frac{1}{2l}\sqrt{\frac{N}{\rho A}} = \left[\frac{p^3 f_n - n^3 f_p}{np(p^2 - n^2)}\right] \times \frac{1}{(1 + 2\delta + 4\delta^2 + 8\delta^3)} \equiv \bar{f}_{CF} \times \phi^{\frac{1}{2}} \tag{43}$$

in which $\bar{f}_{CF} \equiv (p^3 f_n - n^3 f_p)/np(p^2 - n^2)$ is defined as the equivalent frequency of fundamental mode associated with the fixed-fixed model, and ϕ serves as an additional factor to account for the effect of boundary constraints. Consequently, a rigorous formula for evaluating cable force can be proposed as

$$N = 4(\rho A)l^2\left[\frac{p^3 f_n - n^3 f_p}{np(p^2 - n^2)}\right]^2\left[\frac{1}{(1 + 2\delta + 4\delta^2 + 8\delta^3)}\right]^2 = [4(\rho A)l^2 \bar{f}_{CF}^2] \times \phi \tag{44}$$

with $\phi = \left[\frac{1}{(1 + 2\delta + 4\delta^2 + 8\delta^3)}\right]^2$

It is clear that the formula for the fixed-fixed model raises again the problem about the need of evaluation values of ϕ and δ as well. To fulfill this need, another useful relation as shown in Eq. (45) can also be deduced from the simply support beam model in a similar way by cancelling out the axial force in Eq. (33).

$$\bar{f}_B \equiv \sqrt{\frac{p^2 f_n^2 - n^2 f_p^2}{n^2 p^2 (p^2 - n^2)}} = \frac{\pi}{2l^2}\sqrt{\frac{EI}{\rho A}} \tag{45}$$

in which $\bar{f}_B$ can be treated as an equivalent fundamental frequency of flexural vibration of beam. Eq. (45) depicts that the relation between flexural stiffness and mass density can also be established by calculating the value of $\bar{f}_B$ from two specific mode frequencies. As a result, the dimensionless factor δ defined by Eq. (29) can also be approximated by two mode frequencies in a familiar form after substituting the force and stiffness terms with Eqs. (42) and (45), as shown in Eq. (46).

$$\delta = \sqrt{EI/TL^2} \cong \frac{\bar{f}_B}{\pi \bar{f}_C} = \frac{1}{\pi}\sqrt{\frac{p^2 f_n^2 - n^2 f_p^2}{n^4 f_p^2 - p^4 f_n^2}} \equiv \delta_{eq} \tag{46}$$

Although the equivalent δ_{eq} in Eq. (46) is derived based on the simply supported beam model, it provides an optional way of roughly determining the reasonable value for the dimensionless factor δ, and thus it is especially useful when data of flexural rigidity and cable force are not reliable or remain unknowns.

3.2 Bridge structure

Except for special-purposed analysis associated with certain cable-related dynamics, linear dynamic analysis of a cable-stayed bridge can be separated into two parts of analysis, namely stay cables and bridge structure. It is generally accepted that the additional consideration of stay cables in structural modeling has limited influence on the bridge responses, while the cable response may expose dynamic characteristics of the bridge structure. Since the structural system of most cable-stayed bridges consists of regular members of long spans/lengths, modeling with a continuous formulation can be beneficial to the analysis task due to the significant reduction in the number of elements used. The formulation shown in this article contains the assumption of constant cross section which implies that a member with variable cross sectional properties would have to be simulated with multiple divided segments, each still with constant properties. The bridge models described in the following sections are thus modeled as a combination of prismatic members with or without axial forces regardless that the model includes stay cables or not. Using the formulation described for the general flexural members, computer programs were implemented to perform dynamic analysis of 2-D (plane-) and 3-D (space-) frames. The numbers of nodal degrees of freedom of the 1-D line element used for the two types of frames are respectively three (i.e., axial + in-plane flexural motions) and six (i.e., axial + torsional + two flexural motions).

3.2.1 frame model

To perform reasonable simulation for realistic cable-stayed bridges, the computer programs developed in this work are capable of including effects due to axial forces and distributed properties including masses and restraints (springs and dashpots). In a 2-D model, the bridge is simplified as a plane frame. In a 3-D model, the bridge is modeled as a space frame with appropriate amount of lateral members to roughly account for the overall lateral and torsional stiffness due to the out-of-plane motions.

3.2.2 types of responses

After the total dynamic stiffness matrix has been assembled, the equilibrium can be solved for each specific frequency. According to the nature of excitations, the programs developed can simulate two types of dynamic responses. The first type simulates responses due to prescribed ground motions in which the Fourier transform of the support motions are used as input. Eq. (47) shows the equilibrium equations. The subscripts F and R refer to free and restrained nodal displacements, and S_P and U_G refer to the condensed foundation stiffness matrix and the specified support excitations.

$$
\begin{bmatrix} S_{FF} & S_{FR} \\ S_{RF} & S_{RR}+S_P^* \end{bmatrix} \begin{bmatrix} \ddot{U}_F \\ \ddot{U}_R \end{bmatrix} = \begin{bmatrix} 0 \\ S_P^* \ddot{U}_G \end{bmatrix} \tag{47}
$$

It should be noted that this implies that kinematic interaction effects are being neglected. It is assumed that the motions at the top of the foundation would be the same that would occur at that level of the soil without any foundation. At each frequency, the free nodal accelerations are found by solving Eq. (47), the corresponding relative nodal displacements can next be obtained. The second type of excitation simulates responses due to external forces such as point impacting or loads at multiple locations. In this case, the nodal displacements can be directly solved from the equilibrium equations.

After the nodal displacements have been obtained, the displacements at any desired location can be calculated and the corresponding support reactions and the member forces can also be computed. Finally, the time histories associated with these responses can be obtained using the inverse Fast Fourier transform technique.

It is worth noting that the continuous formulation in the frequency domain allows one to directly determine the transfer function, rather than convert from the response histories, thus it provides a more accurate and efficient way to assess the relative importance of different frequency components of motion.

4. Examples of numerical modeling

Numerical models, in which a realistic 3-span cable-stayed bridge as shown in Fig. 2 was modeled as 2-D and 3-D symmetric frames using the proposed continuous formulation, are used to illustrate the potential of the formulae in accessing the dynamic characteristics of the cable-stayed bridge. Both 2-D and 3-D models included two types of simulations, the complete ones contain frame structure and cables while the simplified ones only model frame structure. For the complete models,

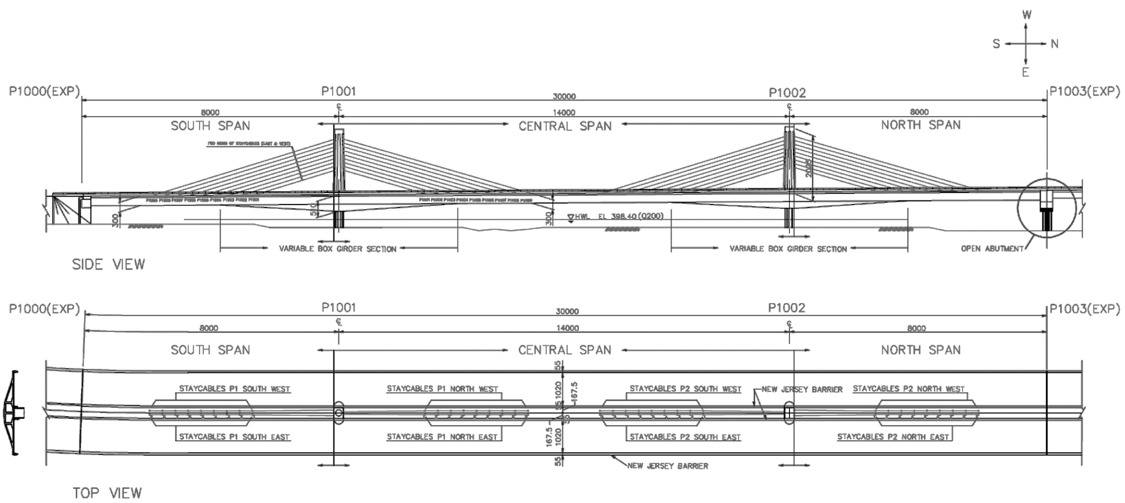

Fig. 2 Configuration of modeled bridge

the bridge members were separated into segments according to the layout of stay cables and thus the number of elements used in the simulation is relatively high. For the simplified models, the bridge members were divided into as few segments as possible so that the efficiency of the formulation can be manifested. The bridge was selected because experimental results associated with certain field tests are available so that comparison between numerical and experimental results can also be made.

For the simplified models, the entire three spans were divided into 12 elements in the 2-D case, 3 for each side and 6 for central. The gradually varying depth of the box girder near piers was roughly simulated with two segments. In the 3-D case, the deck was longitudinally modeled as three parallel lines of girders, each line consists of 12 elements as in the 2-D case. Between the central and the two edge girders there are 26 lateral elements linking nodes at the same longitudinal location. The tapered pylons and uniform piers were all simulated with single segment in which properties at mid-height of the pylon were used.

For the 2-D complete models, the entire three spans contain 40 elements, 10 for each side and 20 for central, and the pylon also consists of 10 elements due to the cable layout. The number of cable elements in the complete models is 72 (2 pairs of 36). For both 2-D and 3-D models, the general properties used are

$$\begin{cases} E = 3.21 \times 10^{10} \mathrm{N/m^2}, \; \nu = 0.2, \; \kappa = \dfrac{5}{6} \\ \rho = 2400 \ \mathrm{kg/m^3}, \; Damping = 0.02 \end{cases}$$

And the displacement boundary conditions were; two ends of the deck are pinned and the bottoms of two piers are fixed.

The main purpose of this study was to conduct parametric studies with generic bridges rather than attempting to duplicate the actual dynamic response of any particular case. The details about the general properties used for the various models are skipped in this paper and yet they can relatively represent the simulated bridge, and data of the 2-D models and their evolved 3-D ones are consistent at least for the in-plane motion along the longitudinal direction.

4.1 Example-1 : impact responses of 2-D model

To illustrate the ability of the formulation to reproduce vertical vibration characteristics in a bridge deck, the case of a side span subjected to an impulse due to sudden stop of a truck near the mid-span of the first span was considered. Fig. 3 shows the transfer functions of the displacements recorded at the mid-span locations of the first (south) and central spans obtained with the direct continuous formulation. The consideration of cables in the model causes the natural modes slightly shift to higher frequencies yet the difference is limited. Therefore, the cables can be neglected when dealing with dynamic characteristic associated with bridge frames. Fig. 3(c) shows, in logarithm scale, the typical transfer function of a cable and that of the deck where the cable is connected to. It is clear that the data recorded at the cable contains the characteristics associated with the deck yet the transfer function is predominantly controlled by cable vibration.

Fig. 4 shows the modal deflections due to this particular loading case for the first two flexural modes, which are associated with the first four peaks indicated in Fig. 3(a). As can be expected,

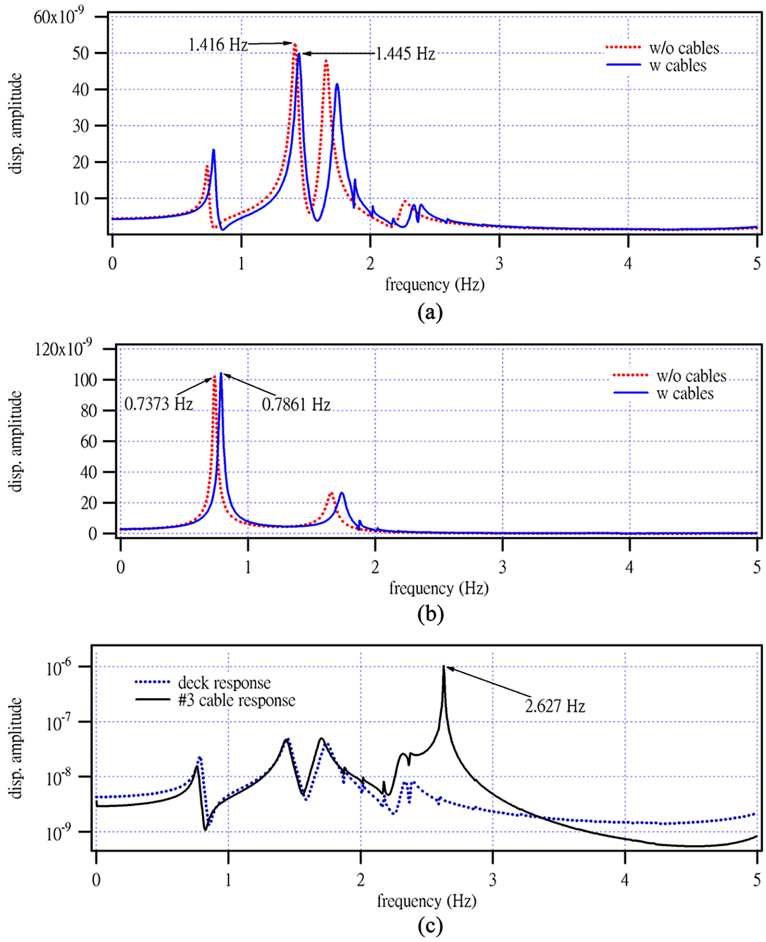

Fig. 3 Transfer functions of 2-D complete models under an impact load: (a) displacement at mid-span of the 1st span (south), (b) displacement at mid-span of the central span and (c) displacement at middle of the #3 cable

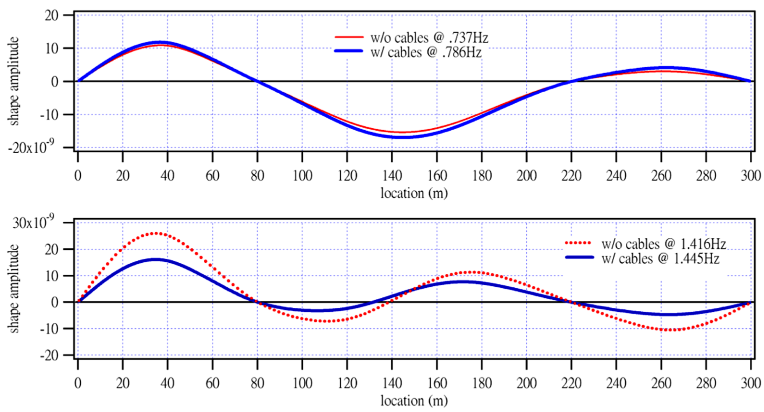

Fig. 4 Response shapes of deck associated with the case of Fig. 3(a)

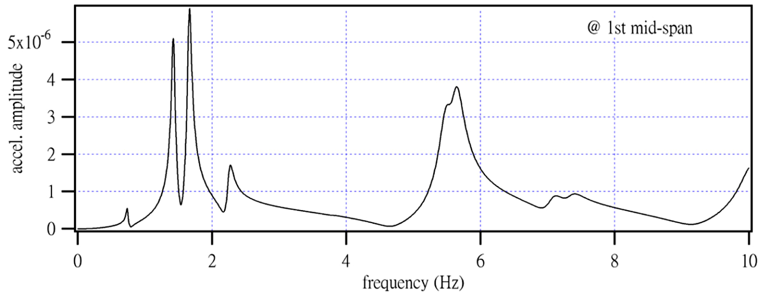

(a)

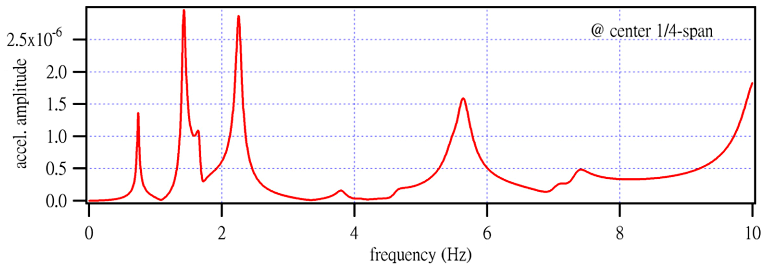

(b)

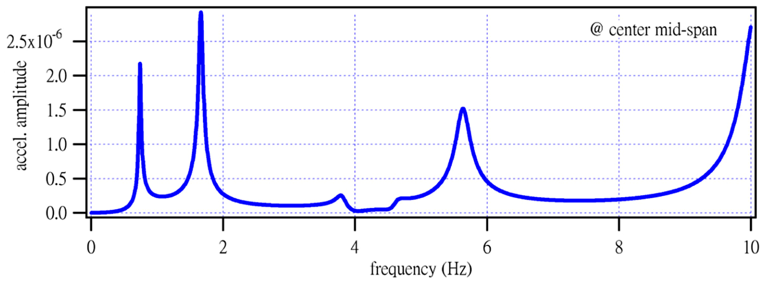

(c)

Fig. 5 Transfer functions of 2-D simplified model under an impact load: (a) acceleration at mid-span of the 1st span (south), (b) acceleration at 1/4th-span of the central span and (c) acceleration at mid-span of the central span

including cables in the model slightly affects the response amplitudes and natural frequencies but not the mode shapes. As a result, modeling of cables can indeed be neglected when only the response of the bridge frame is concerned. This would result in a significant improvement in the computational efficiency since models without cables can be simulated with least number of elements depending on the how we treat the tapered portion of the bridge members.

Fig. 5 shows the result obtained with the simplified model for the same impact problem in which Figs. 5(a) to 5(c) correspond to responses at mid-span of the first span, 1/4th span and mid-span of the central span, respectively. Except that displacement responses are replaced by the acceleration responses in order to clearly show frequency peaks, Figs. 5(a) and 5(c) show similar transfer functions as those obtained by more elements in Fig. 3. It should be noted that a span can be simulated with just one element provided the assumption of uniform cross section for the entire span is used. Fig. 6 shows the corresponding modal deflection shapes due to the particular loading for the first four modes observed from Fig. 5. These modal shapes can be easily related to either symmetric or asymmetric mode of the in-plane flexural motion of the frame.

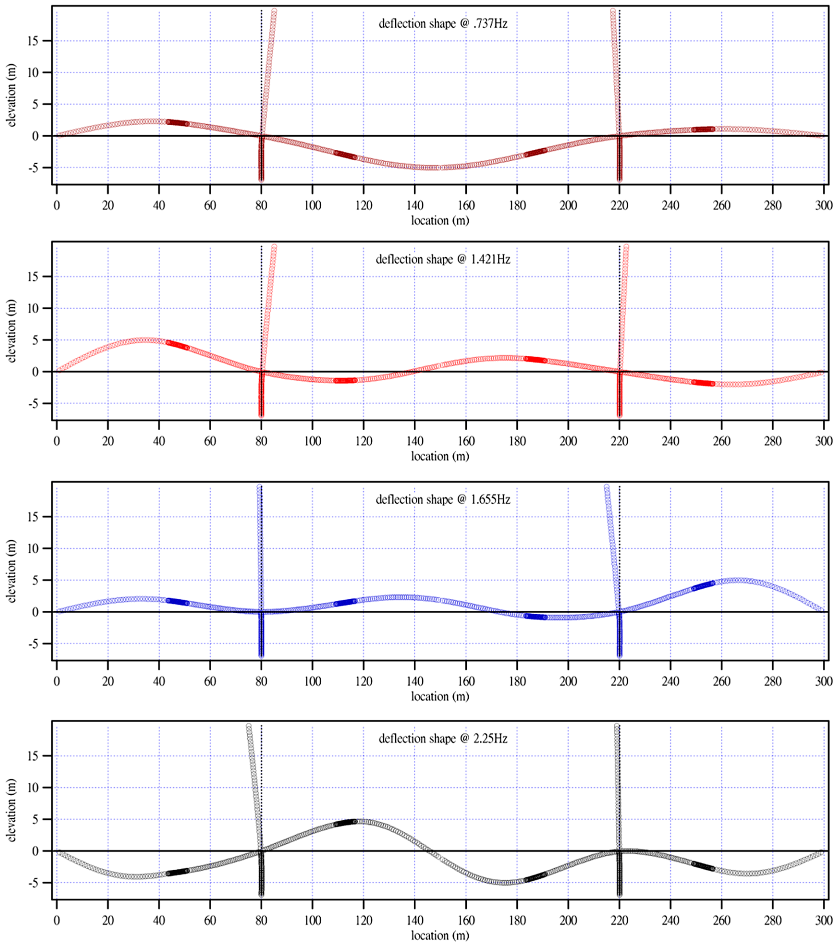

Fig. 6 Response shapes of 2-D simplified model associated with the case of Fig. 5(a)

4.2 Example-2 : seismic responses of 3-D model

To demonstrate the usefulness of the 3-D model, the case of a simplified 3-D model with specified vertical ground motion applied at supports is used as an example. Fig. 7 shows the transfer functions associated with mid-span locations due to uniform vertical support motion in which plots (a) and (b) correspond to the center line and the edge line of bridge deck, respectively. Comparing curves in Fig. 7(a) and Fig. 5, it can be seen that the in-plane motions depicted by the 2-D and 3-D models are generally consistent while the additional mass and stiffness due to adding lateral elements in the 3-D model leads to somehow more complicated curves. From Fig. 7(b), it is obvious that the additional three degrees of freedom of the 3-D model recover more vibration modes than the fundamental 2-D ones.

To manifest further the practicality of the continuous formulation in studying the linear responses of cable-stayed bridges, the 3-D model was also studied by subjecting it to realistic ground motions, such as a significant vertical component of the Northridge Earthquake as shown in Fig. 8(a) where the peak acceleration is as high as 0.54 g. Fig. 8(b) shows the time history of the displacement

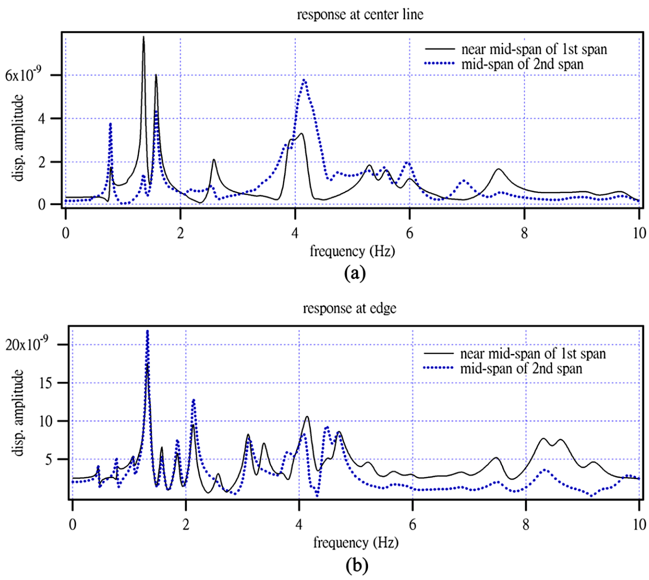

Fig. 7 Transfer functions of 3-D simplified model under vertical ground motion: (a) response at mid-span of the 1st and central spans (along center of deck) and (b) response at mid-span of the 1st and central spans (along edge of deck)

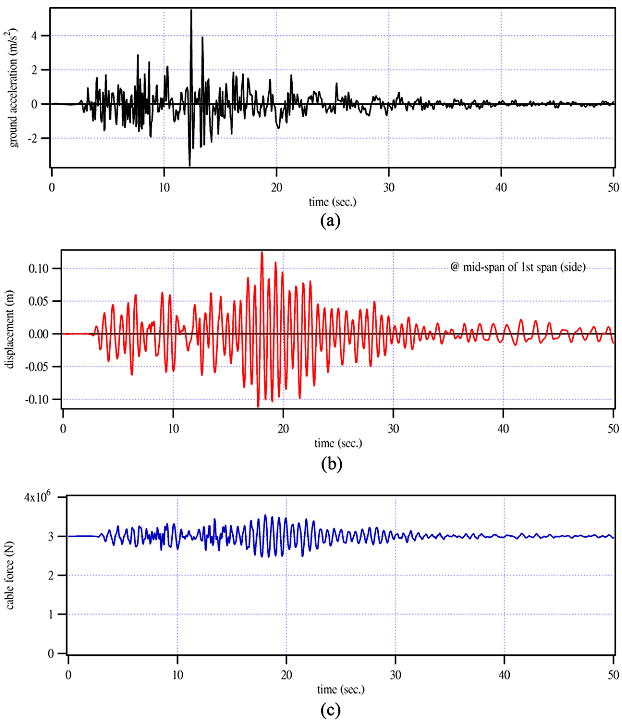

Fig. 8 Response histories of 3-D model due to a vertical earthquake: (a) ground motion with peak acceleration 0.54 g, (b) displacement response at the edge of mid-span of the 1st span and (c) typical force history in cables

recorded at the mid-span of the first (south) span along the edge line of the deck, which is obtained with the transfer function described in Fig. 7(b) multiplied by the frequency components of the ground motion in Fig. 8(a) together with the inverse Fast Fourier Transform to get results in the time domain.

Besides, Fig. 8(c) shows, as another example of related analysis, the typical time response of cable forces due to the described ground motion. In this particular example, one can clearly see the variation of the induced seismic force in the cable is relatively significant thus it can be concluded the assumption of constant axial forces in cables might not be reasonable when bridges are under significant ground motions.

5. Examples of field applications

5.1 Case-1 : verification of cable parameters

The proposed methodology of determining cable force using multiple mode frequencies was put to test with field data obtained from velocimeters. The stay cables are composed of casing pipes with a total of thirty one 7-wired strands of 15.2 mm diameter. The vibration was recorded under normal traffic excitation. Results associated with various cables of identical design length match well and it was concluded the stressing forces can be practically recovered by the proposed formula. For demonstration purpose, the results shown in this example correspond to the case with a design length of 55 m. The assumed mass per unit length (ρA) and the flexural rigidity (EI) of the cable can be reasonably estimated from strand layout and properties of the individual strand as 33.75 kg/m and 1.02 MN-m^2. The dimensionless factor δ, as defined by Eq. (29), associated with this particular set of cables is about 0.01 under their design loads.

Table 1 summarizes the corresponding results for the four sets of cables. Although the equivalent frequencies defined in the previously section 3.1.2, f_C , f_{CF} and f_B, can be calculated using any set of two arbitrary mode frequencies, the values listed in the table were consistently calculated based on the first and fourth modes for each cable in order to provide an insight into the average efficiency of the proposed formulas. It can be seen that results obtained by Eqs. (44) and (46) where EI values are not required agree well with those obtained by Eqs. (39) and (29) which requires precise value of EI. Consequently, it is experimentally evident that the proposed approach of using formulas with two arbitrary mode frequencies can be equally as good as its original counterpart.

Table 1 Comparison of cable forces using different formulas

Set #	f_1 (Hz)	f_4 (Hz)	N_0 (MN)	N_1 w/EI (MN)	N_2 w/δ_{eq} (MN)	N_2/N_1 (%)
1	2.64	10.53	2.8464	2.7225	2.7303	100.3%
2	2.66	10.32	2.8897	2.7649	2.6995	97.6%
3	2.62	10.29	2.8035	2.6805	2.6615	99.3%
4	2.60	9.88	2.7608	2.6388	2.6284	99.6%
Applicable formulas :			Eq. (23)	Eqs. (39) and (29)	Eqs. (44) and (46)	

5.2 Case-2 : verification of vibration modes

As described in the section of numerical examples, the mode frequencies of the simulated 3-span cable-stayed bridge can be reproduced by the mentioned 2-D and 3-D model via analyzing the transfer functions and response shapes associated with the appropriate excitations. This approach is as effective as what is normally done in a traditional FEM analysis in which mode parameters are solved with the eigenvalue analysis. Since conditions of long term traffic normally satisfy the assumption of equal distribution of loading in both the frequency and space domains, field data obtained from ambient vibrations due to long term traffic excitations, such as those in an FDD (frequency domain decomposition) analysis, are expected to match the theoretical mode shapes of an appropriate model. There are, however, circumstances that the real excitations might be different from the ideal one, as a result, certain test results may look questionable when comparing with the analytical solutions of an eigenvalue problem.

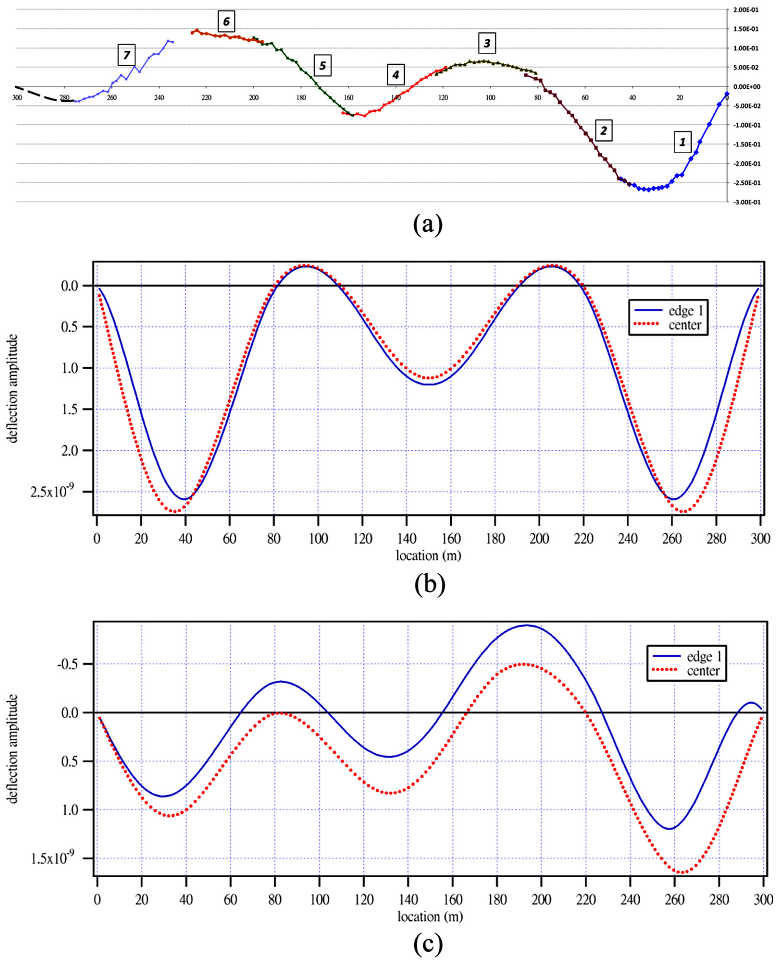

Fig. 9 Comparison between FDD mode shape and response shapes by numerical modeling: (a) FDD mode shape, (b) analytical mode shape (symmetrically flexural model) and (c) response shape due to a set of unbalanced modal load

For instance, Fig. 9(a) shows an experimentally extracted mode shape (FDD result) obtained from the vertical displacement histories along one edge of bridge deck. The response was recorded using a Microwave Interferometer under a long term traffic loading. For this particular mode, the vibration is predominantly flexural vibration and thus the profiles of theoretical mode shapes along the center line and edge line of the bridge deck are almost identical as shown in Fig. 9(b). It is obvious that the difference between the response shapes of the FDD and the numerical results are apparent, which raised a question to the analyst whether the test data is valid or not. After examining the in-situ traffic condition, it was pointed out that the traffic flows were quite unbalanced in the two opposite directions during the testing period, thus the assumption of uniform excitation due to traffic loading appears to be deviated from the real condition. It is interesting to note that, by applying an unbalanced type of modal loads to the 3-D model, the resulting response shapes may become similar to the test one. For example, Fig. 9(c) shows the shapes corresponding to assigning different magnitudes of a specific load pattern at the two sides along the bridge deck, a ratio of two to one was arbitrarily chosen in this particular case. It should also be noted that the reasonable shape happens only at/near the correct mode frequency.

By comparing the solid line in Fig. 9(c) with the test curve in Fig. 9(a), one can clearly see the improved similarity between the two, especially the trends near the two pier locations, namely 80 m and 220 m. Consequently, the test data were then verified as valid with the help of the above comparing procedure. Finally, as a brief summary regarding the above field application, the convenience of using the continuous formulation to generate reliable responses in the frequency domain makes it very easy and effectively to verify related test results by a special-purposed computer program implemented with such formulation.

5.3 Case-3 : scanning a group of stay cables

In addition to monitoring cable vibrations with traditional instrumentations like velocimeters and accelerometers, Microwave Interferometer can also be used to simultaneously scan multiple cables of a cable group. Fig. 10(a) shows as an example a plot containing certain frequency spectra associated with ambient vibration for the nine cables of the same cable group. In practice, each spectrum was arbitrarily normalized so that all curves have comparable peak amplitudes in the same plot. By simulating the cable responses using the 2-D model with a specific excitation pattern, the normalized spectra of the test data can be effectively and reasonably reproduced by the computer program as shown in Fig. 10(b) where each curve was normalized to the same peak amplitude. In addition to the nine normalized peaks, it can be observed from both plots that there are three peaks occurred within lower frequency range, the relatively minor one below 1 Hz and two other peaks near 2 Hz. These peaks are clearly associated with the three modes of the predominantly flexural vibrations of the bridge deck. As a result, such a cable spectrum also carries dynamic characteristics of the bridge deck and thus serves as supplementary information in an assessment task.

Owing to the high computational efficiency of the continuous formulation in obtaining the frequency spectra, the structural properties used for the simulated model can be quickly revised and the stress level of cables can be reasonably determined almost instantly. Although each cable of a group can be easily analyzed individually, simultaneous analysis using a bridge model by adjusting model properties provides one with a better picture of the overall behavior of the cable group and that of the bridge as well.

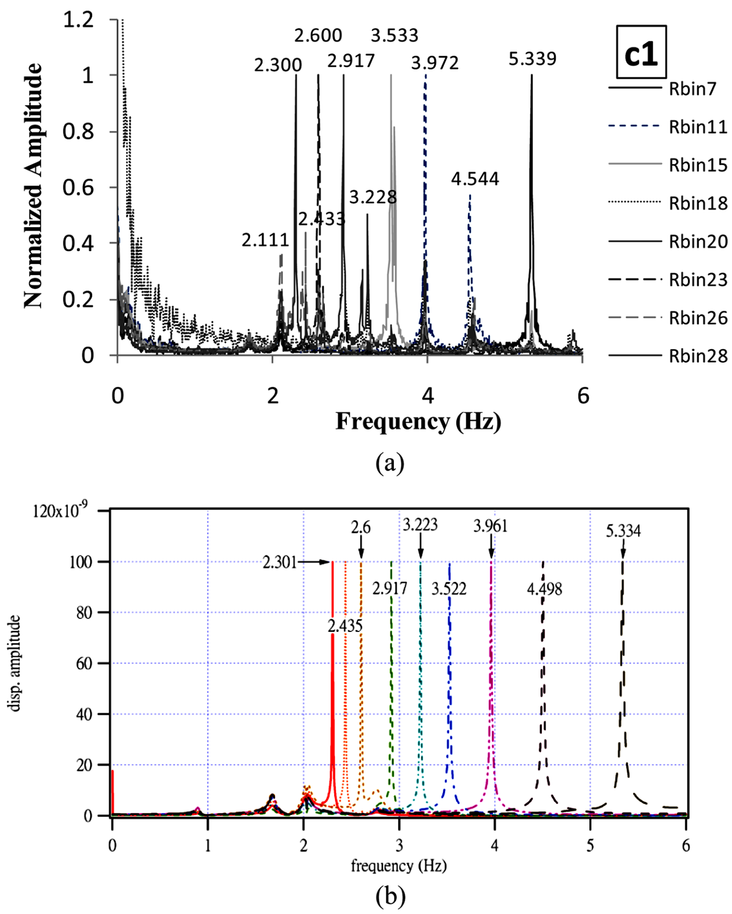

Fig. 10 Comparison between normalized cable spectra: (a) experimental data and (b) numerical simulation using 2-D model

6. Conclusions

This paper presents the use of continuous formulation of 1-D member to verify experimental results of a cable-stayed bridge, in which test data were obtained by in situ instruments including those recorded by a newly developed non-contacting technique, the microwave interferometer. The solution scheme associated with the dynamic analysis of the target bridge includes the implementation of the continuous formulation into computer programs which can carry out 2-D or 3-D simulation for frames with cables, and the use of an innovative back calculation technique to access the axial force of tensioned cables.

The dynamic analysis in the frequency domain using the continuous formulation, on one hand, has the advantage of providing direct computation of the transfer functions, rather than converting from response histories. On the other hand, the use of dynamic stiffness matrices of members with distributed properties not only provides high accuracy for high frequency excitations but also directly calculates rigorous response shapes regardless the degree of discretization in the FE model.

Regarding the determination of cable forces, the proposed formula allows one to carry out rigorous analysis using frequencies of two arbitrary modes of vibration without the need of flexural stiffness. The application of such alternative formula to the field test data confirmed that the proposed approach is capable of predicting cable forces of a cable-stay bridge in good agreements with those analytical values obtained by the original formula. As a result, it is concluded that the proposed formula can be practically useful in cross examining results obtained from other main effective methods.

It is also worth noting that, the use of a versatile monitoring device such as the Microwave Interferometer together with the advantage of carrying out numerical modeling using an effective computer program in the frequency domain allows the authors to speed up the related assessment task in which the delay due to verification of modal data can be greatly reduced.

Acknowledgements

The work is partly supported by the research project funded by China Engineering Consultants, INC, of Taiwan. The authors wish to thank the CECI for its financial support.

References

Ali, M.R. and Okabayashi, T. (2011), "System identification of highway bridges from ambient vibration using subspace stochastic realization theories", *Earthq. Struct*., **2**(2), 189-206.

Banerjee, J.R. and William, F.W. (1994), "An exact dynamic stiffness matrix for coupled extentional-torsional vibration of structural members", *Comput. Struct*., **50**(2), 161-166.

Banerjee, J.R. and William, F.W. (1994), "Coupled bending-torsional dynamic stiffness matrix for an axially loaded Timoshenko beam elements", *Int. J. Solids Struct*., **31**, 749-762.

Bhagwat, M., Sasmal, S., Novák, B. and Upadhyay, A. (2011), "Investigations on seismic response of two span cable-stayed bridges", *Earthq. Struct*., **2**(4), 337-356.

Cheng, C.C., Hsu, K.T. and Yu, C.P. (2010), "Evaluation of the dynamic characteristics of an extradosed bridge using Microwave Interferometer", Proceedings of 2nd Symposium on Life-Cycle Civil Engineering (IALCCE2010), Taiwan.

Cheng, C.C., Yu, C.P., Hsu, K.T. and Wang, C.Y. (2010), "Evaluation of the integrity of a simply supported bridge using Microwave Interferometer", Proceedings of 4th Asian Concrete Federation International Conference (ACF2010), Taipei, Taiwan.

Dai, W., Yu, C.P. and Roesset, J.M. (2007), "Dynamic stiffness matrices for analyses in the frequency domain", *Comput. Aided Civil Infrastruct. E*., **22**(4), 265-281.

Dai, W. (2005), *Evaluation of base isolation and soil structure interaction effects on seismic response of bridge*, Ph.D. dissertation, Texas A&M University, College Station.

Doyle, J.F. (1997), *Wave propagation in structures - spectral analysis using Fast Discrete Fourier Transform*, Springer-Verlay.

Latona, R.W. (1969), *Analysis of building frames for natural frequencies and natural mode shapes*, Inter American Program, Civil Engineering Department, MIT.

Papaleontiou, C.G. (1992), *Dynamic analysis of building structures under combined horizontal and vertical vibrations*, Doctoral Dissertation, University of Texas at Austin.

Wenzel, H. and Pichler, D. (2005), *Ambient vibration monitoring*, John Wiley & Sons, London, 193-198.

Yu, C.P. (1996), *Effect of vertical earthquake components on bridge responses*, Doctoral Dissertation, University of Texas at Austin.

Yu, C.P. (1992), *Application of the hybrid-frequency-time-domain method to morison's equation*, Master Thesis, University of Texas at Austin.

Yu, C.P. and Roesset, J.M. (2001), "Dynamic stiffness matrices for linear members with distributed mass", *Tamkang J. Sci. Eng.*, **4**(4), 253-264.

Yu, C.P., Cheng, C.C. and Chiang, C.H. (2011), "Alternative determination of cable forces using flexural theory of axially loaded member", Proceedings of Smart Structures and Materials & Nondestructive Evaluation and Health Monitoring : Nondestructive Characterization for Composite Materials, Aerospace Engineering, Civil Infrastructure, and Homeland Security 2011 (SPIE), San Diego, CA.

SA